The Pyramidal Electric Transducer:

A DC to RF Converter for the Capture of Atmospheric Electrostatic Energy

Peter Grandics*

Abstract

We have found that the dimensional ratios of the Great Pyramid of Giza (GPG) express the key ratios of an AC voltage sine wave as well as ratios of the Fibonacci number. As pyramidal horn antennas are suitable for the detection of short-pulse waveforms, we reasoned that the shape of GPG could embody a time domain, wideband antenna for atmospheric electrostatic discharge (ESD) impulses. This hypothesis has subsequently been confirmed. We have further found that the pyramidal antenna, modeled on the GPG, can couple into the atmosphere and transfer the power of ESD impulses into a novel lumped-element resonant circuit that converts the random impulses into regular series of exponentially decaying sinusoidal wave trains. Thus, ESD impulses can be transformed into an alternating current of predictable frequency. This system could become a source of renewable electric power by utilizing the electrical activity of the atmosphere.

Introduction

Atmospheric electricity manifests as a buildup of electrostatic energy, a phenomenon that continuously electrifies our environment.[1] In the global atmospheric-electrical circuit, the Earth's surface is negatively charged while the atmosphere is positively charged.[2] The voltage gradient between the Earth's surface and the ionosphere is believed to be maintained by the electrical activity of the troposphere as well as the solar wind-coupled magnetospheric dynamo.[3]

It is difficult to estimate the electric power of thunderstorms, as they typically maintain a steady-state electrical structure during their lifespan[4] despite charge losses from lightning, corona discharges, precipitation, and turbulence. Even with this gap in our understanding of thunderstorm electrification processes, a rough estimate of the magnitude of power generated by thunderstorms can be derived as follows: Thunderstorms can be traced by monitoring lightning activity, more than 90% of which occurs over landmasses, primarily in Central Africa, the South Central United States, and the Amazon Basin.[5] A medium-sized thunderstorm (about 200 km diameter) with intra-cloud voltages of about 100 MV[6] and a precipitation current of about 20 nA/m^2 can generate[7,8] at least 6.28×10^{10} W. Assuming 2,300 active thunderstorms at any given moment,[9] the estimated average total power output of thunderstorm activity is approximately 1.44×10^{14} W. A hurricane's power generation is estimated at about 10^{14} W;[10] in comparison, the total power generation capacity of the world is only 3.625×10^{12} W,[11] a fraction of the power generated in the troposphere by thunderstorm activity. This suggests that the density of atmospheric electrical activity may be high enough to tap, and indicates that atmospheric electricity, if harnessed, could meet all the energy needs of mankind.

Atmospheric electrostatic discharge (ESD) impulses are random and of short duration (nanosecond range) as well as of wide frequency of occurrence. Antennas capable of handling similar short-pulse waveforms can be found in radar systems, where they are called the pyramidal horn antennas.

Intriguingly, popular scientific literature describes inexplicable electromagnetic phenomena under scaled-down replicas of the Great Pyramid of Giza.[12] These phenomena showed a variability that made its interpretation difficult. We hypothesized that these findings were possibly due to natural fluctuations in the atmospheric electrostatic field detected by the GPG as a time domain, wideband antenna. Therefore, we have investigated whether an antenna modeled on the GPG would capture ESD impulses and if these random impulses could subsequently be converted into an AC voltage sine waveform of predictable frequency. This would allow a direct conversion of the potential energy of an electrostatic field into an alternating current, making atmospheric electrostatic charges a possible source of commercial power generation.

Methods and Results

Previously, we reported that a charged pyramidal-shaped capacitor converts ESD impulses into a high-frequency signal that can be detected in an insulated coil placed in proximity of the capacitor plate.[13] Such structure is similar to a transverse electromagnetic antenna (TEM)[14] as well as the pyramidal horn antenna suitable for the detection of impulse events of short duration.

Here, we report on further developments with this system[15] including tracing energy transfer across system components. A laboratory van der Graaf generator (VDG) was used to generate an atmospheric electrostatic field, and Tektronix TPS2024 as well as TDS3054 digital oscilloscopes were used for signal acquisition and analysis. Swept signal analyses were performed by using Wavetek 185 and 187 signal generators.

We first analyzed the dimensional ratios of the GPG and

found that it incorporates key ratios of an AC voltage sine waveform as well as three Fibonacci number ratios (Table 1).

We note that the pyramidal unit cell constants are a function of π and ø. Key sine wave parameters are resonant with the base length and height of the GPG, suggesting that the pyramid may scale up volumetrically as an antenna/electric transducer. The Fibonacci number appears in association with side dimensions (shape factor). The mathematical relationship between π and ø may indicate a coupling between geometrical form and electrical properties. As our pyramidal electric transducer modeled on the GPG may function as a time domain, wideband antenna, it is possible that the ratios displayed in the GPG are sufficient for the design of these types of antennas. Therefore, the GPG may demonstrate a "universal" antenna design.

To investigate this possibility, a logarithmic sweep was performed on a 1 foot base length pyramid from 500 Hz to 5 MHz at 10 msec sweep speed by using a Wavetek 185 signal generator (Figure 1). The pyramid was placed inside a cylindrical metallic emitter (52 cm diameter, 26 cm high with 0.3 mm wall thickness) to account for the fact that atmospheric ESD impulses are received omni-directionally.

Experimental setup:

The 50Ω output of the signal generator is connected to the cylindrical emitter.
Channel 1 is the signal measurement (pyramid).
Channel 4 is the sweep signal control voltage (ramp waveform of 10ms period).
The oscilloscope trace shows a wide bandwidth response demonstrating that the 1 foot base length pyramid indeed functions as a wideband antenna.

Table 1. The summary of the main mean dimensions of the Great Pyramid of Giza[16] and an analysis of its ratios.

Dimension	meter	royal cubit
L (base)	230.35	440
height	146.71	280
slope	186.52	356
edge	219.21	418
D (base diagonal)	325.76	622.25

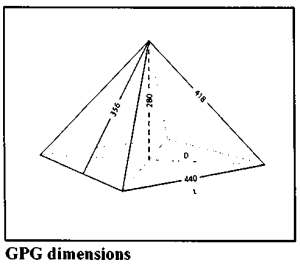

GPG dimensions

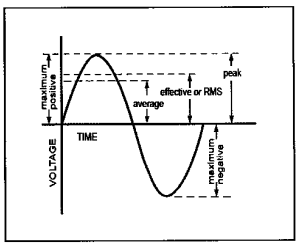

Sine wave

GPG dimensional ratios	Key sine wave ratios
280/440=0.6363=2/π	AVE/PEAK=0.6363=2/π
440/622.25=0.707	RMS/PEAK=0.707
280x622.25/440x440=0.9	AVE/RMS=0.9
280/D/2=0.9	AVE/RMS=0.9

Fibonacci number ratios in GPG	
356/L/2=1.618	ø
356/418=0.80905	ø/2
356/280=1.271	√ø

π/4=1/√ø

For the power transmission studies, we used the same pyramidal antenna/charge accumulation element modeled on the GPG.[13] The electrostatic field in air produces ESD impulses on the conductive pyramid's external surface. A coil wound with insulated wire on a conductive cylindrical substrate (coilform) is attached electrically and mechanically to the conducting surface of the pyramid near its apex. The coil is connected in parallel with an external capacitor to provide a specific resonant frequency.

A secondary coil of smaller diameter (coil 2) of a greater length and larger number of turns is positioned coaxially within the first coil and serves as a resonant step-up transformer winding inductively coupled with coil 1 (Figure 2). After charging the pyramid capacitor, the signal measured on coil 2 leads is an exponentially damped sinusoidal waveform at regular periodic intervals (Figure 3).

The pyramidal electric transducer is capable of absorbing ESD impulses from an electrostatic field generated by a laboratory VDG (Figure 4). Periodic discharge events were detected at a distance of 1 m between the pyramid and the VDG. The electrostatic field strength was measured by using a Monroe 244 electrostatic voltmeter and found to be about 3 kV/m, much less than the field strength observed during thunderstorms at ground level (10 kV/m or more).[17]

A load may be connected to coil 2 to draw power from the system. The load may be a resistor, a rectifier or storage

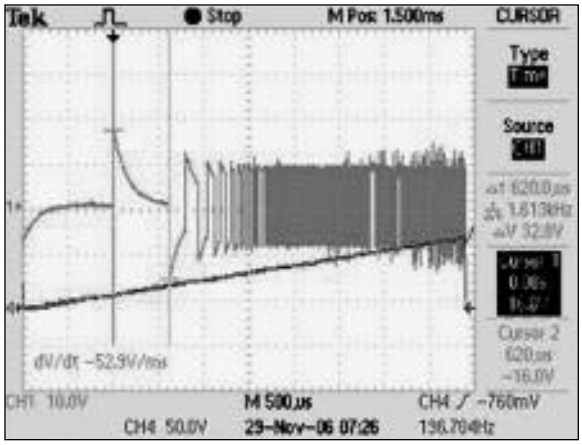

Figure 1. The spectral response of the 1 foot base length pyramidal antenna.

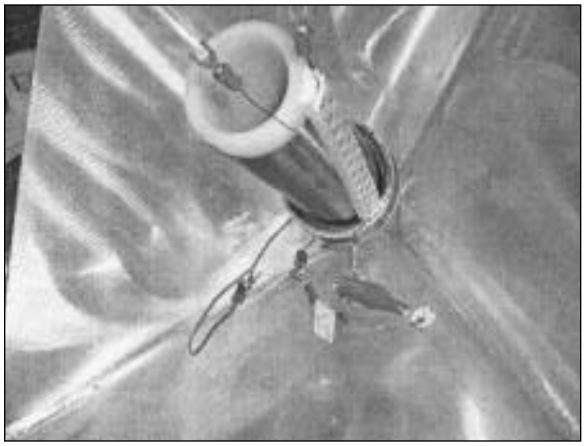
Figure 2. Placement of coils inside the pyramidal charge collector with resonance capacitor.

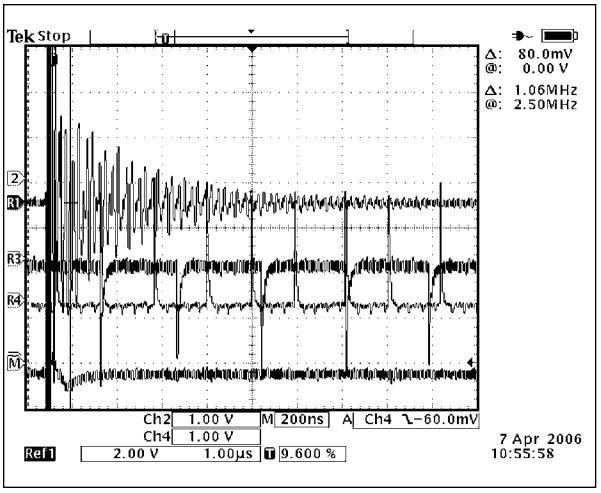

Figure 3. The pyramid coil 2 signal measured by oscilloscope.

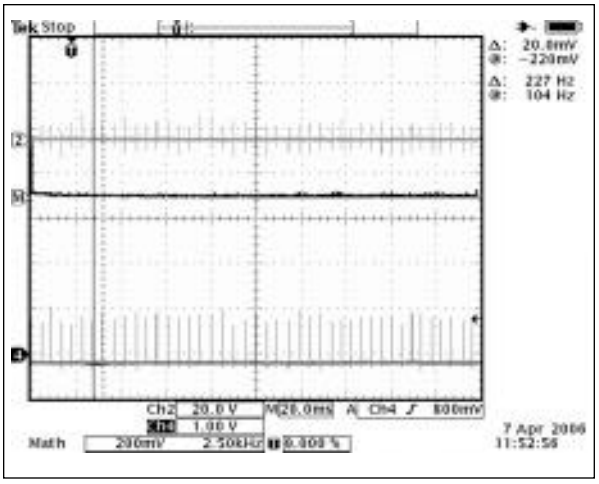

Figure 4. Pulse train of discharge events.

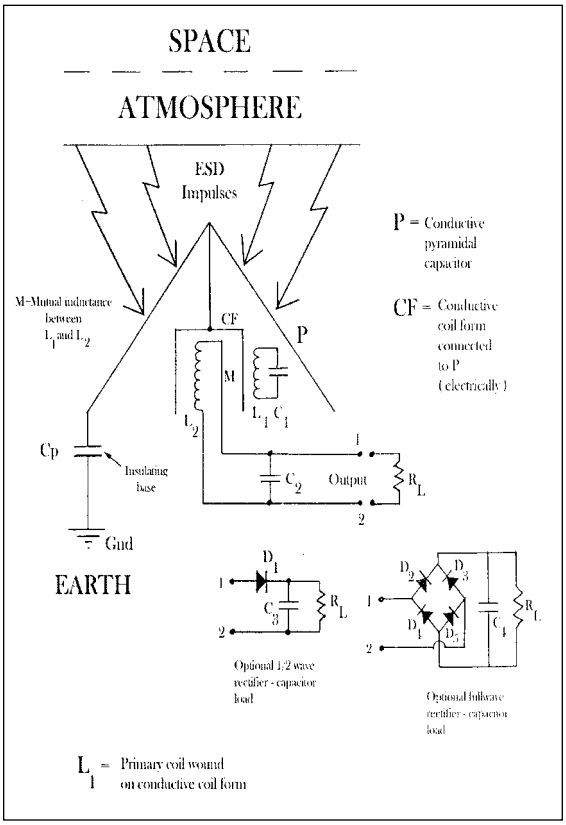

Figure 5. The pyramidal electric transducer circuit model.

capacitor powering a DC load, or simply a fluorescent tube serving as an AC load with threshold nonlinearity (Figure 5).

The circuit diagram of the pyramidal electric transducer is shown in Figure 5. The pyramidal charge accumulation element (P), placed on an insulating base, couples to the atmosphere and serves as an antenna for ESD impulses. It also forms a capacitor with the Earth ground.

The pyramid's body is attached electrically and mechanically to a lumped-element resonant circuit (LEC) that converts ESD impulses into an RF signal (Figures 3 and 6). The LEC, a combination of three capacitive elements and one inductive element (Figure 6), is capable of charging as well as periodic resonant discharging. The L_2 secondary coil (coil 2) wound on a nonconductive coilform serves as a step-up transformer and forms a resonant circuit with the C_2 capacitance. The secondary coil output can be connected to a rectifier-capacitor-load resistance.

The energy transfer between the LEC and coil 2 was studied, as shown in Figure 6. The coils were activated with a logarithmic sweep from 50 kHz to 50 MHz at 100 millisecond sweep speed. The scope trace (Figure 7) indicates approximately 1 octave per horizontal division, from left (50 kHz) to right (50 MHz). The signal, a sine wave with 5 V peak amplitude, is delivered across a 1 kilo-ohm resistor to the unit under test.

Experimental setup:

Channel 1 is the signal measurement (coil 1).
Channel 2 is a second probe (100 Mohm, 10x) attached to coil 2 output wires.
Channel 3 is the sweep frequency marker of the Wavetek 178 signal generator.
Channel 4 is the sweep signal control voltage (ramp waveform of 100 ms period).

With a resonance capacitor (290 pF) across coil 1, the resonance of the coil 2 second peak is detected at about 9.5 MHz. The peak voltage across coil 1 also appears at about at this frequency (Figure 8). By optimally tuning coil 1 peak and coil 2 second peak together, the output can be optimized, *i.e.* maximum power transferred to coil 2 from the sweep generator.

We carried out differential measurements to investigate the energy transfer from coil 1 to coil 2 with the pyramid attached to the coilform and the signal generator output connected to the pyramid. Probe 1 is connected to one side of coil 2 and probe 2 is connected to the other. The probe 2 signal is subtracted from the probe 1 signal to reveal what is happening across coil 2; the middle trace is the difference between the sides of coil 2 (Figure 9).

An energy transfer from coil 1 to coil 2 was shown in the spectral response of the middle trace. It reveals a first resonance at about 6.55 MHz, then zero, then a cascade of other resonances up to about 25 MHz.

Subsequently, we coupled one output lead of coil 1 to the coilform and thus to the pyramid body to make it resonant with coil 1. The differential signal is higher, indicating enhanced energy transfer (Figure 10). We have also investigated whether the geometry of and coil winding on the conductive coilform has an effect in the spectral response seen in coil 2

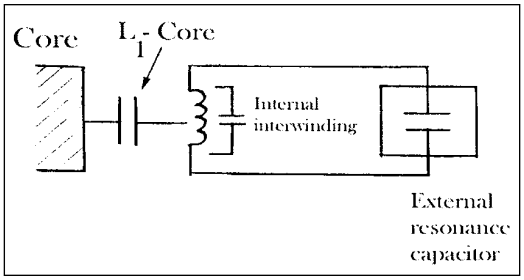

Figure 6. The lumped-element resonant circuit model.

output (Figure 8). For this, a new coilform was made that covered over two-thirds of coil 2 in length, with a 1.3 mm thick, dielectric-filled space left between the coilform and coil 1. Repeating the swept signal analysis of Figure 8, we see that coil 2 draws power from coil 1 at a frequency of about 4.8 MHz; some absorption at a lower frequency peak is also seen (Figure 11). The modified geometry and the extra spacing between the coil 1 winding and coilform may have allowed a higher Q and less coupling to coilform.

Subsequently, we developed another conductive coilform that completely enclosed coil 2. A Teflon heat-shrink sleeve 0.4 mm thick was placed over the entire length of the coilform. An acrylic tube was then placed over the coilform (3.1 mm wall thickness) and held in place with tabs leaving a 1 mm wide air-gap. Coil 1 was wound on the acrylic tube (27 turns) using 20 AWG enamel-coated magnet wire. Repeating the swept signal analysis of Figure 8 produced very high Q peaks from both coils that were well tuned together (Figure 12).

We subsequently set a signal generator (Wavetek 185) producing asymmetrically square-shaped waves (5V) to measure power transfer across the system. Channel 1 showed damped sinusoidal pulse trains starting about 1 V p-p. Channel 2 showed damped sinusoids about 10 V p-p (Figure 13). To measure power into the pyramid, a 10Ω resistor was placed in series with the waveform generator. Voltages were measured at channel 3 (input drive from generator) and channel 4 (after the 10Ω resistor). The math function of the scope was used to subtract channel 4 from channel 3 (Figure 14).

To calculate power into the pyramid, voltage across the 10Ω resistor was multiplied by current through the same resistor (calculated from voltage and resistance). To calculate the power out of coil 2, the voltage across coil 2 was multiplied by the current through the 100kΩ load resistor (calculable from voltage). Power transfer efficiency calculations are shown in Table 2.

We have also repeated this experiment by driving the pyramidal electric transducer with the VDG connected in series with a 10Ω resistor. The power across the system was calculated as above (Table 3). Further optimization is needed in order to increase system efficiency.

Electromagnetic modeling of the power transfer element is shown in Figure 15. The conductive pyramid is electrically coupled to the conductive coilform for coil 1. The coil of conductive wire surrounded by dielectric insulation is coupled to the coilform, mainly by capacitive coupling between the coilform and the individual windings of wire around it, separated by the thickness of the dielectric. Another important factor in the modeling is the coil inter-winding capacitance, determined by the average wire diameter and distance between conductive turns. Likewise, the coil resistance is the total resistance of the wound coil, but it interacts with the coil-to-core incremental capacitance and the inter-winding capacitance.

Although the coil is a continuous system, and an exact model would be represented by a complex integral calculus expression, a simpler "discrete" model can be created by treating the entire coil as a series of single-turn coils, each with its own resistance, per-turn inductance, inter-winding capacitance, and coil-to-core capacitance. The coil is then represented as a series connected set of single-turn elements.

The entire coil-core-resonance system (represented in Figure 6) indicates the total interwinding capacitance, as well as the total coil-to-core capacitance and the total inductance. An external resonance capacitor (a discrete external component) is connected across the coil to provide a resonant frequency determined by the cumulative combination of components affecting the coil properties of inductance, resistance, interwinding capacitance, coil-to-core capacitance, and external capacitance. This provides the basis for calculating the expected performance characteristics of the coil system, comparing it with experimental results, and supporting further optimization of the entire system. This research is ongoing in our laboratory.

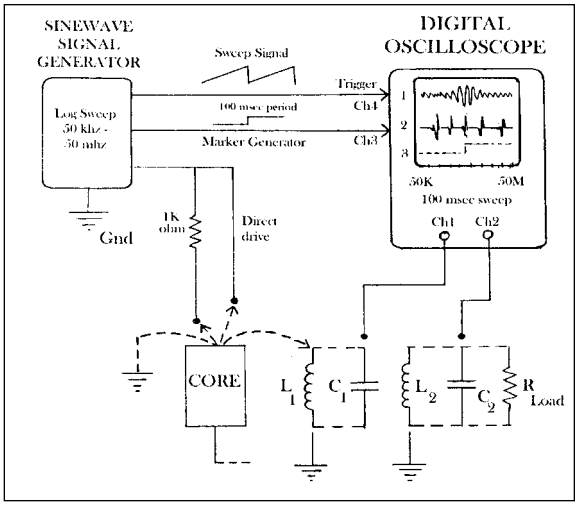

Figure 7. Swept signal analysis setup.

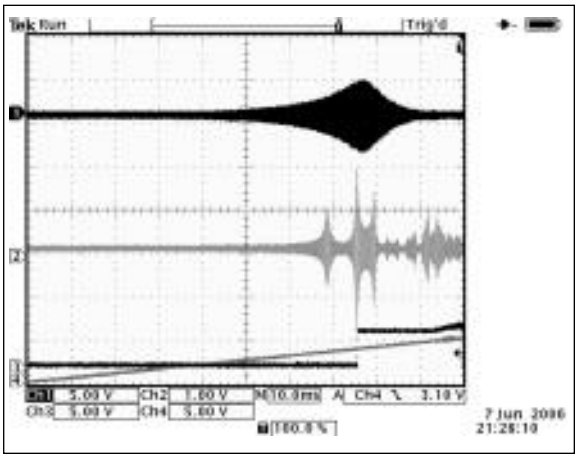
Figure 8. Swept signal analysis of coil resonances and energy transfer.

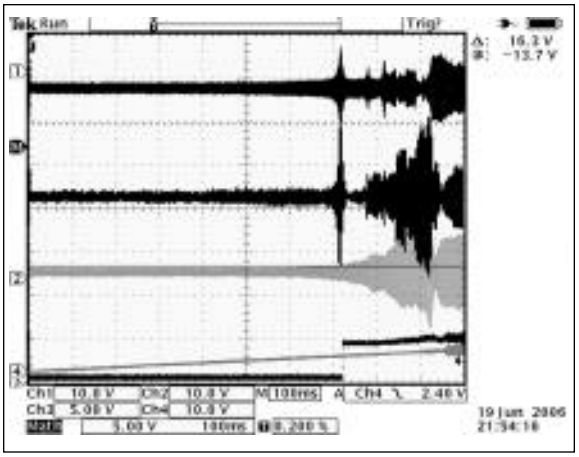
Figure 9. Differential measurement on coil 2.

Discussion

This study demonstrates a novel approach to tap atmospheric electrostatic energy. One intriguing aspect is the shape effect, *i.e.*, the observation that a pyramid-shaped antenna may be optimal for capturing atmospheric ESD impulses.[13] This observation is supported by the sur-

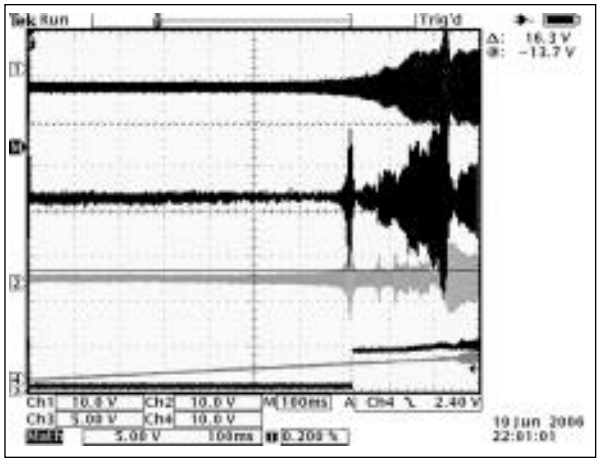

Figure 10. Differential measurement on coil 2 with one lead of coil 1 output connected to the pyramid body.

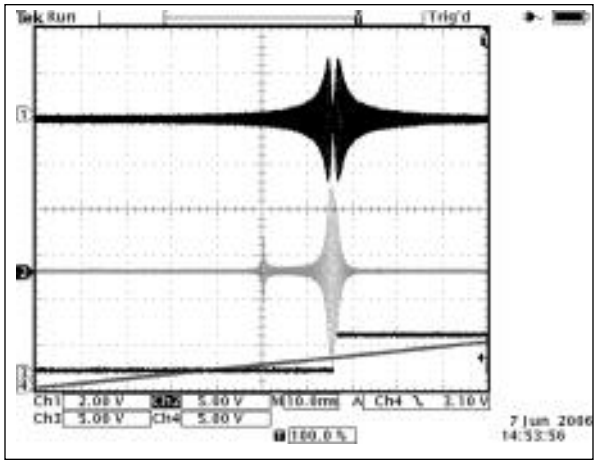

Figure 11. Swept signal analysis of coil resonances and energy transfer with the modified coil form.

prising result of our analysis of the dimensional ratios of the Great Pyramid of Giza, which raises the possibility that its builders were trying to construct a structure that could act as a wideband antenna. This possibility has subsequently been confirmed by measuring the spectral response of a pyramidal antenna modeled on the GPG. Our results also provide an explanation of the inexplicable electromagnetic phenomena observed under scaled-down replicas of the GPG.[12] As vertical atmospheric potential follows a diurnal and seasonal cycle, this explains the variable results reported. Further analysis of this phenomenon will likely advance our understanding of the physical bases of electromagnetism.[18]

ESD impulses are converted into periodic, exponentially decaying sinusoidal wave trains by a novel lumped-element resonant circuit, comprising an insulated coil wound on a conductive cylindrical substrate that is electrically coupled to the pyramid body and is parallel to a resonance capacitor. Connecting one lead of coil 1 to the pyramid body increases energy transfer as the charge accumulation element (pyramid) resonates at the frequency of the LEC. This can have a significant bearing on the ability of the system to attract electrostatic energy. With optimization of the coil system, power transfer efficiencies should be in excess of 90%, as RF transformer design is a well-established field of RF engineering.

Estimating the electric power of thunderstorms that typically maintain a steady-state electrical structure during their lifespan—despite charge losses to lightning, corona discharges, precipitation, and turbulence—is difficult.[4] In fact, precipitation current carries only a portion of the charges present inside the thundercloud. The actual magnitude of electric power generated by thunderstorm activity may exceed global power generator capacity by as much as three orders of magnitude. The geographical concentration of terrestrial thunderstorm activity would facilitate efforts to tap into this large pool of atmospheric energy.

We also propose that the generation of electricity would be commercially practical even in the absence of thunderstorm generators. Holtzworth reported that a large fraction of the ground-ionospheric potential difference of 450 kV can be bridged at a low altitude of 1500 m;[19] at this elevation he measured a short circuit current of 30-50 μA[20] using a short wire mesh charge collector. As the charge-accumulating capacity of the pyramid is directly proportional to its surface area, a sufficiently large pyramid could potentially generate megawatts of power even under fair weather conditions. This activity would be facilitated by an observation reported from Russia.

Radar testing of the space over a 44 m tall fiberglass pyramid located near Moscow[21] revealed a large ionized column of air over the area of the vertical axis of the pyramid. The

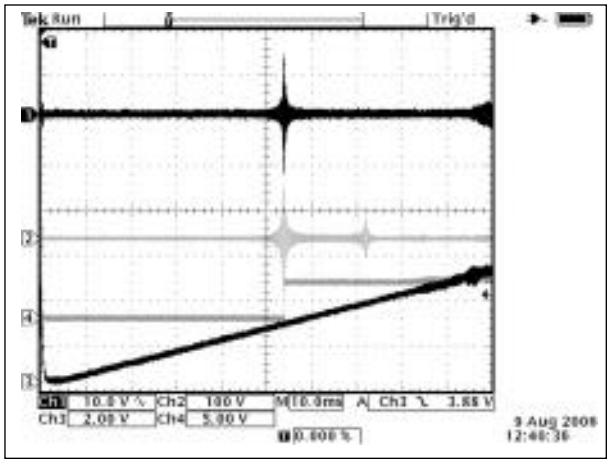

Figure 12. Measurement of resonance coupling with the redesigned coilform.

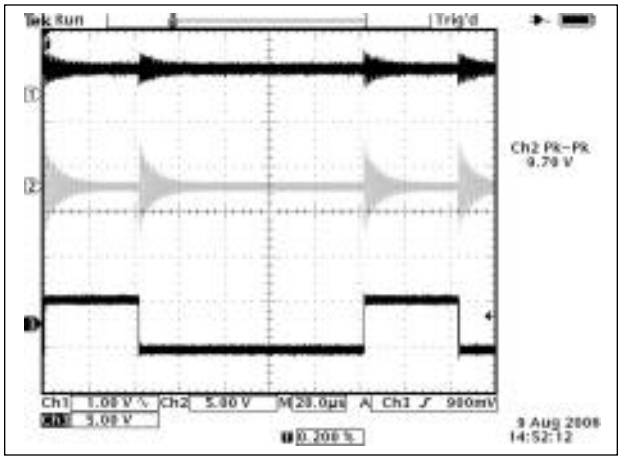

Figure 13. Decaying sinusoidal waveforms generated in coil 1 and coil 2 by asymmetrical square-wave pulsing.

column had a width of about 500 m and reached an altitude of 2 km. It is remarkable that this effect was induced by a nonconductive pyramidal surface, demonstrating a significant degree of atmospheric ionization even under fair weather conditions. Thus, a suitably sized pyramid may open a low impedance path to higher elevations of relatively conductive atmospheric domains.

This effect would likely be amplified by coupling the first resonant circuit to the charge accumulation element pyramid body. Thus, its RF output, by enhancing the attraction of charges to the pyramidal electric transducer by a similar ionization of the atmosphere, could reach a matter of miles into the troposphere with a full-scale power generator pyramid.

The Russian study also noted a reduction in the frequency of lightning in the vicinity of the pyramid. This is easy to interpret in the context of our observations. As electrification of thunderclouds drive severe weather including lightning phenomena, depleting charges from thunderclouds would reduce both lightning activity as well as atmospheric turbulence. With the increasing frequency of hurricanes and other severe weather phenomena, installation of properly sized pyramidal electric transducers in hurricane-prone heavily populated areas could become more than just vehicles of power generation: they could have additional benefits by saving both lives and property.

In conclusion, possibly thousands of terawatts of power are generated in the troposphere by thunderstorms. A pyramidal structure, with its optimal geometry and construction, can act as a suitable charge sink, capturing this electric power and preventing its dissipation.

A power-generator pyramid with an approximately 34,000 m^2 base surface area, a height of 100 m, and a conductive surface would provide a far more effective charge sink than the surrounding ground surface. Charge capture would be aided by internal resonant circuits to increase operational efficiency under fair weather conditions. Groups of several pyramidal electric transducers could be placed within specific geographical areas, thus combining their charge collection capacity.

Global warming caused by anthropogenic greenhouse gas emissions is now driving major environmental changes that threaten to upset our ecosystem with potentially catastrophic consequences.[22,23] Atmospheric electricity is a renewable, clean energy source that could give humanity an opportunity to begin reversing a dangerous and self-destructive ecological trend, as well as protect important weather-threatened areas from physical harm.

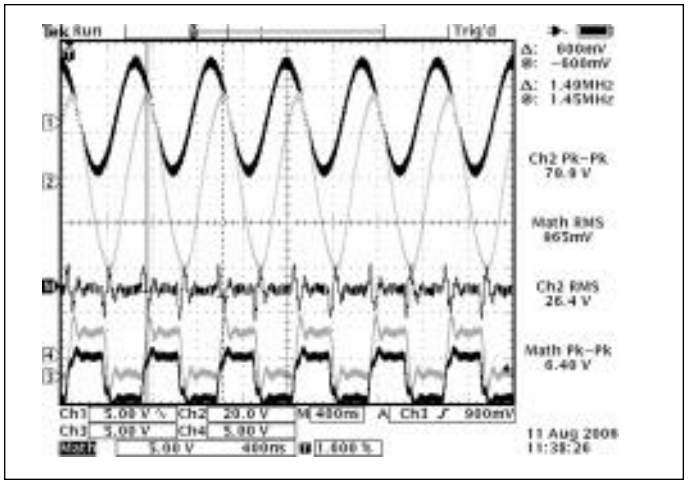

Figure 14. Measurement of power transfer across system.

Table 2. Calculation of power transfer efficiency across the system.

Input power
Math Channel
0.965V RMS; R = 10Ω
Frame time: 4 µsec

$I = 0.965/10 = 9.65 \times 10^{-2}A$
$P = VxI = 0.965 \times 9.65 \times 10^{-2} = 9.312 \times 10^{-2}W$

Output power
Channel 2 (Coil 2 output)
26.4V RMS; R = 100kΩ
Frame time: 4 µsec

$I = 26.4V/100k\Omega = 2.64 \times 10^{-5}A$
$P = VxI = 26.4 \times 2.64 \times 10^{-5}$
$= \mathbf{6.969 \times 10^{-4}W}$

Efficiency (E%)
$E = 6.969 \times 10^{-4}/9.312 \times 10^{-2} =$
$0.7483 \times 10^{-2} \times 100 = \mathbf{0.74\%}$

Table 3. Calculation of power transfer efficiency with VDG driver.

Input power
Math Channel
6.72V RMS; R = 10Ω
Frame time: 100 µsec

$I = 6.72/10 = 0.672A$
$P = VxI = 6.72 \times 0.672 = 4.515W$

Output power
Channel 2 (Coil 2 output)
70.9V RMS; R = 100kΩ
Frame time: 20 µsec

$I = 70.9V/100k\Omega = 7.09 \times 10^{-5}A$
$P = VxI = 70.9 \times 7.09 \times 10^{-5} =$
$5.026 \times 10^{-3}Wx5 = \mathbf{2.513 \times 10^{-2}W}$

Efficiency (E%)
$E = 2.513 \times 10^{-2}/4.515 =$
$0.556 \times 10^{-2} \times 100 = \mathbf{0.55\%}$

Acknowledgement

I thank Mike Beigel from Beigel Technology Corporation for his work with the measurements and his participation in this study. I am also indebted to Mike Beigel and Gregory M. Vogel for their valuable comments and suggestions on the manuscript.

References

1. Anderson, R.V. 1977. In *Electrical Processes in Atmospheres*, H.

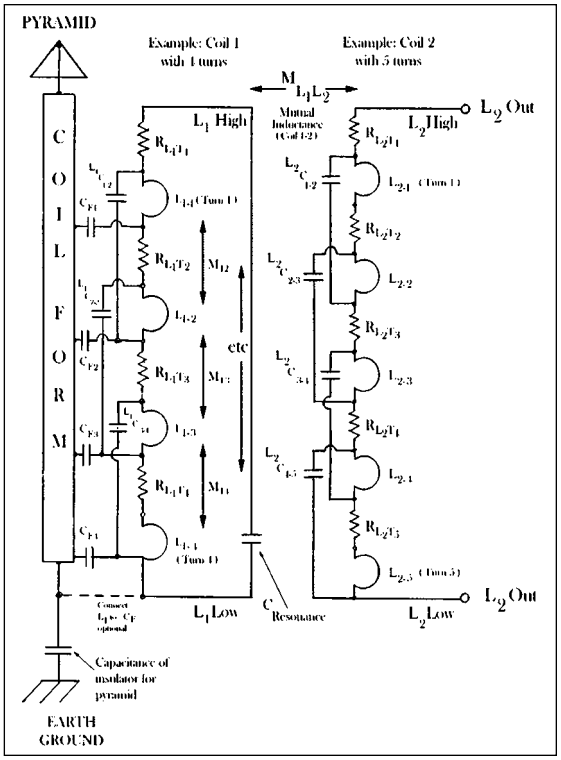

Figure 15. Elements for incremental model of coils and coil form.

Holezalek and R. Reiter, eds., Steinkopff, Darmstadt, pp. 87-99.
2. Feynman, R.P. 1964. *Lectures on Physics*, Addison Wesley, Inc., Palo Alto, California, Vol. 2, Chapter 9.
3. Roble, R.G. and Tzur, I. 1986. In *The Earth's Electrical Environment: Studies in Geophysics*, National Academy Press, Washington, D.C., pp. 206-231.
4. Bateman, M.G., Rust, W.D., Smull, B.F., and Marshall, T.C. 1995. "Precipitation Charge and Size Measurements in the Stratiform Region of Two Mesoscale Convective Systems," *J. Geophys. Res.*, 100, D8, 16341-16356.
5. Miller, T.L. Global lightning activity, online at http://www.ghcc.msfc.nasa.gov/rotating/otd_oval_full.html.
6. Marshall, T.C. and Stolzenburg, M. 2001. "Voltages Inside and Just Above Thunderstorms," *J. Geophys. Res.*, 106, 4757-4768.
7. Christian, H., Holmes, C.R., Bullock, J.W., Gaskell, W., Illingworth, A.J., and Latham, J. 1980. "Airborne and Ground Based Studies of Thunderstorms in the Vicinity of Langmuir Laboratory," *Q.J.R. Meteorol. Soc.*, 106, 159-175.
8. Marshall, T.C. and Winn, W.P. 1982. "Measurements of Charged Precipitation in a New Mexico Thunderstorm: Lower Positive Charge Centers," *J. Geophys. Res.*, 87, 7141-7157.
9. Krumm, H.C. 1962. "Der weltzeitliche Tagesgang der Gewitterhaufigkeit," *Z. Geophys.*, 28, 85-104.
10. Anthes, R.A., Panofsky, H.A., Cahir, J., and Rango, A. 1978. *The Atmosphere*, 2nd ed., Charles E. Merrill, Columbus, Ohio, pp. 442.
11. World Total Electricity Installed Capacity, January 1, 1980-January 1, 2003, Energy Information Administration, http://www.eia.doe.gov/iea/elec.html.
12. http://www.freeweb.hu/piramisfesztival/piramisadatok.htm
13. Grandics, P. 2000. "A Method to Capture Atmospheric Electrostatic Energy," *Proceedings of IEJ-ESA Joint Symposium on Electrostatics*, Kyoto University, Kyoto, Japan, pp. 355-361.
14. Pao, H.-Y. and Poggio, A.J. 1999. "Design of a TEM Waveguide for Ultra-wideband Applications," *Proc. 1999 IEEE APs Int. Symp.*, 3, pp. 1574–1577.
15. Grandics, P. 2006. "A DC to RF Converter for the Capture of Atmospheric Electrostatic Energy," *Proceedings of the 5th Conference of the Societe Francaise D'Electrostatique*, Grenoble, France pp. 279-284.
16. http://www.aiwaz.net/modules.php?name=News&file=article&sid=6
17. Krehbiel, P.R. 1986. In *The Earth's Electrical Environment: Studies in Geophysics*, National Academy Press, Washington D.C., pp. 206-231.
18. Grandics, P. 2007. "The Genesis of Fundamental Forces Acting at a Distance," *Infinite Energy*, 12, 71, 13-24.
19. Holtzworth, R. 1981. "Direct Measurement of Lower Atmospheric Vertical Potential Differences," *Geophys. Res. Letters*, 8, 783-786.
20. Holtzworth, R. Personal communication.
21. http://www.pyramidoflife.com/eng/tests_experiments.html
22. Kerr, R.A. 1999. "Will the Arctic Ocean Lose All Its Ice?" *Science*, 286, pp. 1828.
23. Laxon, S., Peacock, N., and Smith, D. 2003. "High Interannual Variability of Sea Ice Thickness in the Arctic Region," *Nature*, 425, pp. 947-950.

About the Author

Peter Grandics has an MS in chemical engineering and a Ph.D. in biochemical engineering. He has worked in the fields of biomedical research and recently in physics focusing on new energy technologies. He intends to help find answers to our current global energy challenges.

*P.O. Box 130912, Carlsbad, CA 92013
E-mail: pgrandics@earthlink.net